

## Remanufacturing process chain for end-of-life aluminium car body parts: Technical and economic analysis

FARIOLI Daniele<sup>1,a\*</sup>, MURGESE Luca<sup>1,b</sup>, PINARDI Camilla<sup>1,c</sup>,  
KAYA Ertuğrul<sup>1,d</sup> and STRANO Matteo<sup>1e</sup>

<sup>1</sup>Politecnico di Milano, Department of Mechanical Engineering, Via La Masa 1, 20156 Milano, Italy

<sup>a</sup>daniele.farioli@polimi.it, <sup>b</sup>luca.murgese@mail.polimi.it, <sup>c</sup>camilla.pinardi@mail.polimi.it,  
<sup>d</sup>ertugrul.kaya@polimi.it, <sup>e</sup>matteo.strano@polimi.it

**Keywords:** Remanufacturing, Dismantling, Aluminium Sheets, Flattening, Circular Economy

**Abstract.** This paper investigates the potential for remanufacturing aluminium sheets from end-of-life vehicles (ELVs), specifically focusing on car hoods. The study explores various pre-flattening procedures and reshaping techniques, with warm flattening showing promise despite challenges such as paint degradation. A Design of Experiment (DoE) was used to assess the impact of various factors on the flattening process, and Finite Element (FE) simulations were used to validate the experimental findings. An economic feasibility analysis was also conducted, which revealed that while technically feasible, the economic viability of this remanufacturing process is currently challenging due to the high costs compared to purchasing new sheets. However, with the increasing use of aluminium in automotive body panels and potential market shifts, these remanufacturing initiatives could become economically viable in the future, contributing to sustainability goals in the automotive sector.

### Introduction.

Traditional business models follow a “make-use-dispose” approach, but the concept of circulating materials and products, which offers environmental and economic benefits, is gaining popularity. This can be achieved through open-loop or closed-loop supply chains where materials or products are reused, recycled, repurposed, or remanufactured. This paper focuses on the remanufacturing of automotive panels to enable a circular economy of car body panels. Specifically, it analyses the use of a flattening technique on Al-alloy automotive panels as an alternative to conventional recycling by melting. Aluminium, a high-value material, is increasingly used in the automotive sector due to its lightweight and corrosion-resistant properties. Unlike recycling, flattening allows for the reuse of material without remelting, preserving the chemical composition of a specific alloy. There is growing interest in recycling aluminium scrap at temperatures below solidus, known as “melt-less” or solid-state recycling, which offers significant environmental benefits in terms of energy and material savings. The paper provides a comprehensive analysis of flattening as a remanufacturing process, including a technical, economic, and environmental assessment of a case study related to End-of-Life Vehicles (ELVs) aluminium hoods [1], [2].

### Circular Economy in the automotive sector.

The concept of circular economy aims to minimize waste and promote sustainable resource usage by designing products, materials, and systems to maximize their value and longevity. With energy and material consumption rising rapidly, resource constraints have become increasingly critical. Developing closed-loop manufacturing systems is crucial for economic and environmental sustainability, meeting consumer needs, and creating high-skill jobs. In the automotive sector, implementing a circular economy requires adopting Closed-Loop Supply Chain (CLSC) practices,

which include reverse logistics. Unlike traditional open-loop supply chains, CLSC incorporates cradle-to-cradle principles, involving gatekeeping, collection, sorting, and disposal or recovery (e.g., reuse, recycle, refurbish, remanufacture). Implementing CLSC faces challenges, grouped into environmental, cultural, economic, manufacturing and technological, information-related, regulations, managerial, and organizational barriers. However, various facilitating drivers, such as economic, environmental, technical, and political factors, also exist [3]. In the automotive sector, implementing a circular economy relies on adopting Closed-Loop Supply Chain (CLSC) practices, which differ from traditional open-loop supply chains by incorporating reverse logistics. This shift moves from a cradle-to-grave approach to a cradle-to-cradle model. Reverse logistics consists of gatekeeping, collection, sorting, and disposal or recovery (e.g., reuse, recycle, refurbish, remanufacture). However, implementing CLSC faces challenges, including environmental, cultural, economic, manufacturing and technological, information-related, regulations, managerial, and organizational barriers. Despite these challenges, facilitating drivers such as economic, environmental, technical, and political factors exist. In the automotive sector, achieving a perfect CLSC is unlikely due to the complexity of the network and involvement of various actors. Nevertheless, the CLSC in the automotive field mainly involves the forward supply chain network (suppliers, manufacturers, customer clusters) and the reverse chain network (collection centers, recyclers, remanufacturers, dismantlers, shredders, landfills) [4].

The reverse logistics network starts with the collection of ELVs from customer clusters. The owner of a used vehicle who wants to sell it has many opportunities. If the vehicle is in good condition, he/she can decide to sell it to another person, or to a collection centre such as a dealership. If the vehicle is not in good condition, that means it is an ELV, the owner can decide to take it directly to a dismantler or to a collection centre that is in contact with a dismantler. In dismantling centres, cars are depolluted and disassembled, it is decided which parts and materials can be recovered and which must be sent to landfills. In general, the outputs of the dismantling process are used components and hulk, composed of ELV body, chassis, and other structural parts. The hulk is sent to a shredding facility where it is possible to divide all the different materials composing it. Usually, the ferrous and non-ferrous fractions obtained are recycled while the Automotive Shredder Residue (ASR), that is the non-metal fraction obtained, is sent to the landfills.

The objective of the sheet remanufacturing through flattening, the focus of this paper, is to avoid the transfer of ELV aluminium sheets from the dismantlers to the shredders and recyclers. For this reason, it has been necessary to evaluate deeply the existing relations between dismantlers and shredders. These last are complementary figures, the shredder is particularly sensitive to the dismantler's aggressiveness in disassembling the ELV. When only a small percentage of the vehicle is sold as parts, it considerably limits the dismantler's profitability and increases the shredder's profitability. This is particularly true for Al components that have a high economic value. Aluminium, being obtained from bauxite, is a Critical Raw Material (CRM), whose recovery is very important. This is the reason why emphasis is placed on the flattening technique that can be applied to Al-alloy sheets, by either cold or warm reshaping. It consists of using a used metal sheet, cutting out a preform, and forming the sheet again [5]. Remanufacturing activities offer a distinct advantage as they embody the ideal compromise between recycling efforts and the preservation of inherent value.

### **Experimental feasibility study.**

A case study from the automotive sector was selected. It was decided to focus the analysis on car hoods since they are often characterized by extended Al panels. Aluminium hoods are built with inner and outer Al alloy panels, polyurethane foams, and structural tapes. To start the experimental process, three hoods produced in different years and belonging to different car models (Peugeot 407 SW of 2004, Jeep Renegade of 2014, BMW series 5 G30 of 2017) were collected from dismantling

facilities. Disassembling the hoods and cutting them into various sections to generate representative samples were the first operations carried out. The three Al-hoods employed were cut according to Figure 1, which represents only one of the three end-of-life part from which samples were extracted. In total 18 samples made of three different 6000 series Al hoods were obtained. Some of the samples present a mild initial curvature (labelled with “B” in Figure 1); some other included a sharp design line (labelled with “D” in Figure 1, where a change in concavity can be appreciated). The trimming process was performed with an angle grinder because of its precision and reduced energy consumption compared to other methods.

Then, it was necessary to remove the polyurethane foams through a mechanical action. In addition to that, a significant issue arose during the removal of structural tapes, leading to various attempts, including mechanical methods and solvents. The subsequent steps included the paint removal from certain samples: various techniques were taken into consideration. Sandblasting removed the paint but led to deformation issues, attributed to the interaction between residual stresses from the original forming process and the one introduced by this process. Chemical solvents were then employed, demonstrating good efficacy in stripping the paint from the specimen surface.

Later, the specimens were geometrically characterized using a 3D scanner (Artec EVA) and a 2D laser profilometer system (Wenglor MLWI 131), described in Figure 2. Both systems provide as output either an .stl file or a .csv file containing a cloud of data point. Such data were analysed through MATLAB: the software allowed generating a script for automatically determining the local radius of curvature and the maximum height of each specimen profile. After scanning, a 400 tons hydraulic press was employed to reshape the aluminium samples. Such process is meant to cancel out the original curved shape of the samples and providing a flat sheet by applying a pressure through two flat dies.

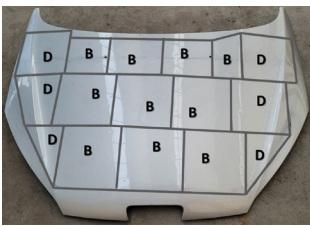


Figure 1. Drawn pattern followed during the cutting.

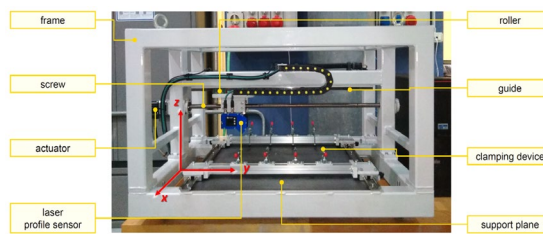


Figure 2. Laser-based profilometer used for 3D scanning the samples.

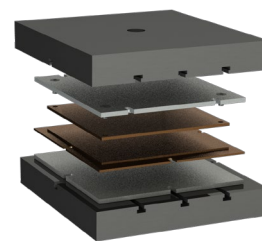


Figure 3. Exploded view of the modular flattening dies.

Flattened panels, once reshaped, can be reused for another purpose, in a circular economy perspective. A modular tooling set has been designed, made of steel 1.2842, divided into four parts as shown in Figure 3. The flattening plates can be heated up to  $T=300\text{ }^{\circ}\text{C}$  to perform warm reshaping. The lower plate is stationary while the upper plate descends and presses the samples with different speeds, with the following sequence:

- 1) First, a rapid descent of the top die occurs, at 80 mm/min;
- 2) Then, the speed is reduced to 25 mm/min until contact with the sample and onset of flattening. This speed is maintained up to a target tonnage is reached;
- 3) Lastly, once reached the target tonnage (i.e. the dwell force, DwF), the position of the upper plate is maintained to press at a constant force onto the sample for a pre-determined time called dwell time ( $\tau$ ).

The temperature of the upper and lower plate can be set and maintained constant by means of 18 electrical resistances (9 for each plate). Knowing the surface area of each specimen, an average dwelling pressure  $P$  is calculated for each operation as the ratio between the tonnage (DwF) and the surface area. A Design of Experiment (DoE) was established to understand the influence of

temperature (T), pressure (P), dwell time ( $\tau$ ), and presence of folds on the flattening process. These parameters were chosen based on their expected influence on the re-forming operation [6]. As previously mentioned, from ELVs parts 18 specimens with initial different geometry have been selected for testing. The selected variables for the analysis included two values of temperature T (25-250 °C), two values of pressure P for the dwelling stage (30-40 MPa), two values of dwell time  $\tau$  (10-20 s, with longer time exclusively for hot-flattened specimens), and the presence of design line as a categorical factor (see Figure 1, samples type “D”). Such values of temperature, pressure, and dwell time were selected after a preliminary experimental campaign not described for sake of simplicity. In fact, such values guaranteed observing significantly different responses and spring-back, allowing capturing the effect of the process parameters, which is the aim of this DoE.

After flattening, specimens were geometrically measured again. Preliminary observations after the hydraulic press operation revealed that cold flattening was less effective, particularly for components with significant curvature. This might be attributed to the spring-back phenomenon and to the fact that being the curvature “large”, not effective plastic deformation is applied while reshaping. A noteworthy observation was made regarding the role of paint in the flattening process. Some painted samples revealed issues during hot flattening, including paint melting, bubbles formation, and generation of gaseous substances as shown in Figure 4. This phenomenon was attributed to pyrolysis, a thermochemical decomposition reaction in a reducing atmosphere. Despite the challenges posed by paint degradation, it was observed that warm flattening allowed for easy removal of the superficial layer of paint without chemical action (Figure 5). This added value to the component, as the E-coating (substrate protective layer) remained unaffected.

To investigate the influence of process parameters, the relationships between independent and dependent variables were examined.

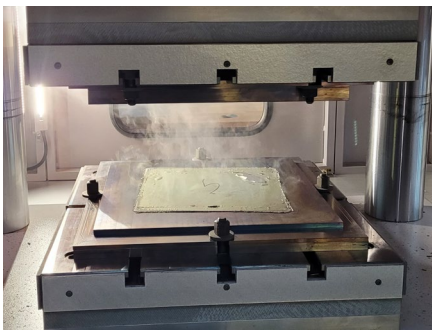


Figure 4. Specimen after warm flattening.

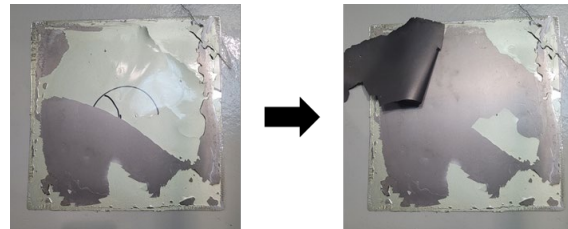


Figure 5. Easier paint detachment if flattening is performed at 250°C.

The beneficial effect of temperature is shown in Figure 6, where the boxplot of the difference between the initial curvature radius and the final curvature radius after flattening is reported. Larger differences imply a more effective flattening operation. The specimens flattened at 250 °C exhibit significantly higher curvature radius differences than those flattened at room temperature. This is clearly due to lowered strength of Al at elevated temperatures. For specimens with a design lines, a significant influence of pressure was also observed, as shown in Figure 7. Samples subjected to higher pressure, surprisingly, exhibit a smaller difference in height, i.e. larger springback. Sometimes the difference is even negative, with a final part which is less flat than the initial part.

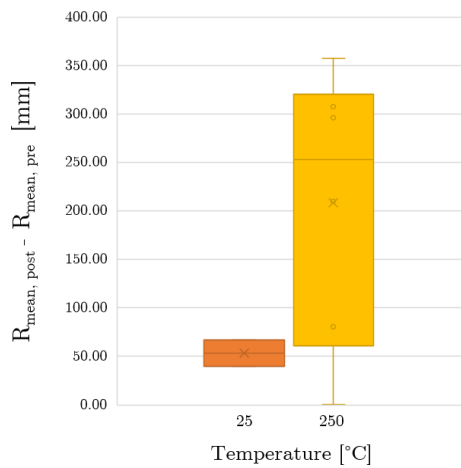


Figure 6. Box-plot of the variation in radius vs.  $T$  with specimens featuring a design line.

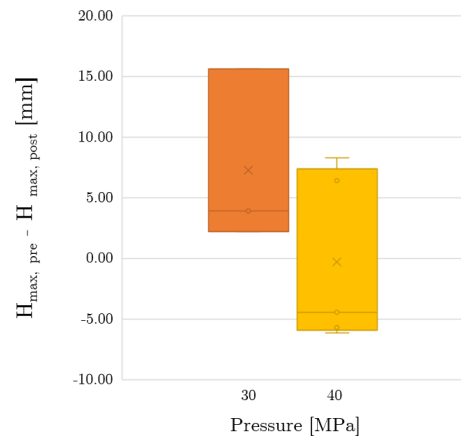


Figure 7. Box-plot of the variation in height vs.  $P$  with specimens featuring a design line.

This is because flattening may induce a U-shaped deformation, or a spring-forward effect, as visible in Figure 8. The spring-forward effect is a consequence of the initial geometry of the sample (Figure 8-a) which is characterized by a design line (not touching the lower plate) and a change in concavity: the red area has a concavity pointing upwards while the green area (where the design line is present) downwards. Furthermore, the curvature radius of the red zone is larger than the green one, making more difficult to enter in the plastic field simply with flat dies, which during flattening are basically applying counter-bending to the material. After dwelling, the central portion of the sample, where the design line was present (Figure 8-c), can deform plastically because of the flattening plates which firstly un-bend and then compress the material through the thickness. The red portion instead, having a larger curvature radius, unbends mainly elastically. Therefore, that portion does not get completely flat and still a curvature pointing upwards exists, leading to a lateral raise of the flange which might be bigger than the initial maximum height pre-flattening. Experimental observations highlighted that the spring-forward phenomenon is typical in parts exhibiting a design line once pressed at higher pressures and warm conditions since temperature can facilitate plastic deformation at the contact to the design lines. Besides, a higher contact pressure ensures a better heat transfer between the warm dies and the part, making the unbending of the central fold easier. Lastly, dwell time  $\tau$  could ensure a longer or shorter heat transfer by contact directly from dies to the part, emphasizing or not the spring-forward effect. As for  $\tau$ , distinct behaviours were observed in specimens with and without design lines (Figure 9).

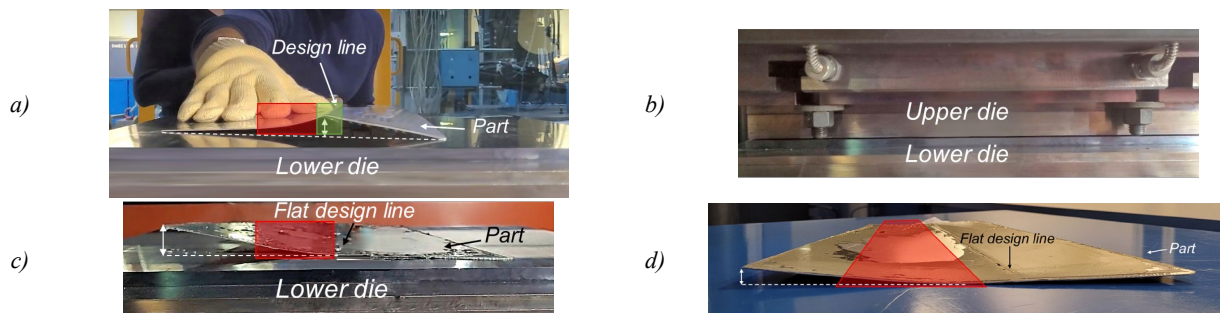


Figure 8. a) Positioning of the part. b) Flattening. c) Spring-forward effect. d) Residual “U” shape effect, or spring-forward.



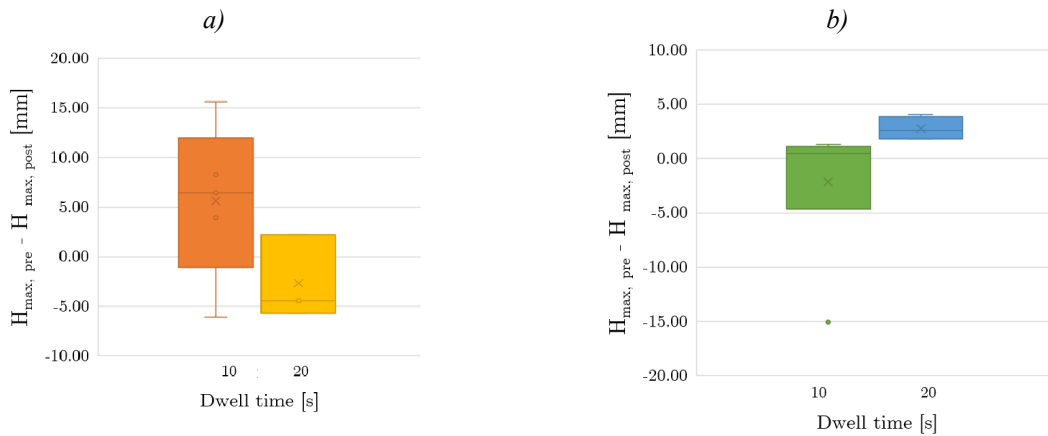


Figure 9. Box-plot of the variation in height vs.  $t$  for specimens with (up) and without (down) a design line.

For long dwell times, specimens with design lines exhibit improvements in curvature radius but deterioration in terms of maximum height. When flattening is performed at high temperature with a long dwelling time, thermal distortions are induced. In conclusion, the mechanism of flattening is complex because of several factors, which might interact with each other (Figure 10): geometry, residual stresses, thermal distortions and process parameters are fundamental actors.

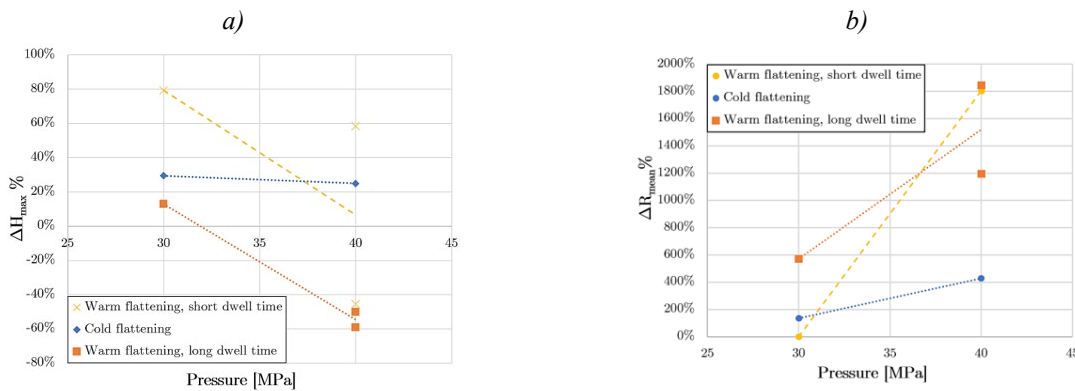


Figure 10. Interaction plots between factors ( $P$ ,  $T$ ,  $\tau$ ) onto the response variables  $\Delta H_{max}\%$  (top) and  $\Delta R_{mean}\%$  (bottom) for specimens with a design line.

Because of the intrinsic complexity of this process, in the next section of this article it is presented a Finite Element (FE) simulation of one case study tested, with the aim of understanding if flattening, spring-back and part shape can be predicted digitally.

**Simulation of the flattening process.**

This section presents the results obtained from an FE simulation that digitally replicates the entire remanufacturing process chain. Altair Inspire Form software was employed for this activity. The material employed in the simulation is the Al 6016 (as in the real case). It was modelled with elastoplastic behaviour. The software adopts a yielding criterion according to a three-parameter Barlatt model ( $R_{00}=0,686$ ,  $R_{45}=0,5$ ,  $R_{90}=0,666$ ) with exponent  $m=8$ . The plastic field of the material follows a power law model with coefficient  $K=400$  MPa and hardening exponent  $n=0,213$ . Altair Inspire Form uses an explicit FE solver and all the forming stages were modelled: initial cold forming of the hood, trimming of the specimen, cold flattening, and spring-back (Figure 12). Prior to the final simulation (Figure 13), a convergence analysis of the mesh size was carried out. In the end, the initial flat blank was modelled with quadrilateral shell elements with edge size equal to 4 mm. No remeshing or adaptative algorithms were implemented. The flattening simulation

revealed low plastic strain near the design line (Figure 13), suggesting that the mechanical properties of the component were only partially affected. The values of the elastic springback obtained from the FE simulation (i.e. the nodal coordinates of the meshed part) were imported in MATLAB and then compared to the ones measured onto the real specimen. Despite minor deviations, there was notable correspondence between actual and virtual profiles (Figure 11). This result validates the use of FE simulation as a tool for predicting accurately the component final morphology.

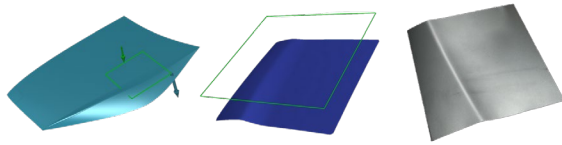


Figure 12. From left to right: output of the forming process; output of the trimming operation of one part extracted from Figure 1; 3D scan with Artec EVA of the real sample pre-flattening.

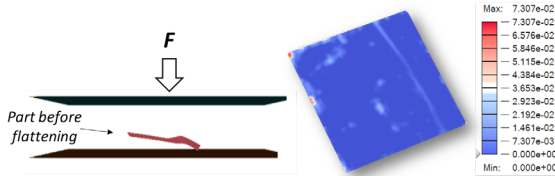


Figure 13. From left to right: simulative setup for flattening; plastic strain distribution of the part after flattening and spring-back.

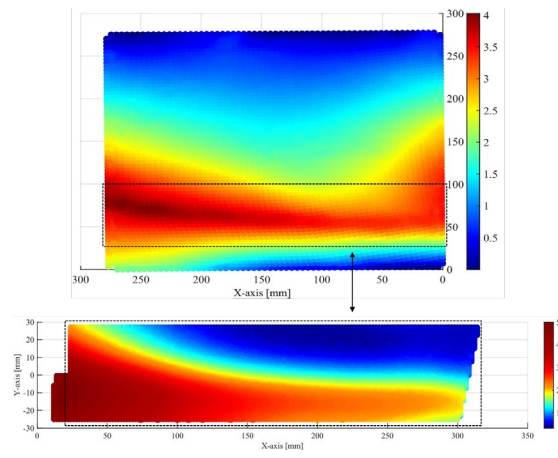


Figure 11. Up: Height profile of the scanned portion from the real specimen. Down: Height profile of the simulated specimen. The dashed rectangle corresponds to the same regions.

**Economic feasibility.**

To perform an economic analysis, it is necessary to evaluate which will be the future aluminium sheet quantity recoverable from ELVs. Analysing UNRAE (Unione Nazionale Rappresentati Autoveicoli Esteri) data from 1990 to 2022, the values of car registrations and car radiations were forecasted for future years (Figure 14). The data collected showed that reasonably the newest car models (last 5/10 years), after an average of 18 years of usage are dismantled. Therefore, it was assumed for simplicity, that 2022 car registrations are related to 2040 car radiations, and 2025 car registrations to 2043 car radiations. The missing point is knowing the car registered in 2025. For that a “scenario-based” analysis was employed allowing the forecast of car registrations of 2025. It was then possible to compare car radiations of 2040 and 2043 and the number of cars dismantled in 2040 and 2043 was obtained.

The data resulting from the forecasts allowed to understand the values of the sales volumes and of the dismantling volumes, however, they had to be transformed into Al sheet fluxes. To do that, the 59 best-selling cars of 2022 were considered as reference, classified according to their segment, and analysed to determine which bodywork components they have in aluminium. Such 59 best-selling car models represent the 72.9% of the entire market share in Italy of sold cars in 2022. For sake of simplicity, the first 20 top sold car models are reported in Table 1.

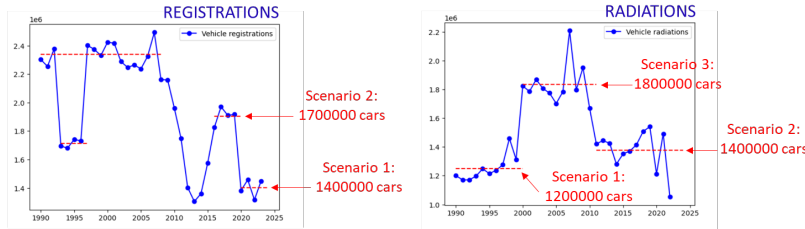


Figure 14. Analysis of the Italian car registration and radiations in the last 30 years from UNRAE.

Number	Brand	Model	Segment	2022 Sales
1	Fiat	Panda	A	105,384
2	Lancia	Ypsilon	B	40,970
3	Fiat	500	A	33,996
4	Dacia	Sandero	B	33,922
5	Citroen	C3	B	31,879
6	Jeep	Renegade	C	29,954
7	Ford	Puma	B	29,479
8	Toyota	Yaris	B	27,813
9	Toyota	Yaris Cross	B	26,023
10	Peugeot	208	B	25,827
11	Renault	Captur	B	25,456
12	Dacia	Duster	C	25,245
13	Volkswagen	T-Roc	C	25,053
14	Fiat	500X	C	22,244
15	Jeep	Compass	C	22,151
16	Volkswagen	T-Cross	B	20,851
17	Opel	Corso	B	17,839
18	Renault	Clio	B	17,839
19	Peugeot	3008	C	17,138
20	Peugeot	2008	B	16,449

Table 1. First top 20 sold car models in Italy (2022).






Segment A	Segment B	Segment C	Segment D
 UP	 Polo	 Golf	 Tiguan
	 T-cross	 T-roc	 Passat

Table 2. Car model considered as “reference” for the automotive market in Italy. Courtesy of Volkswagen.

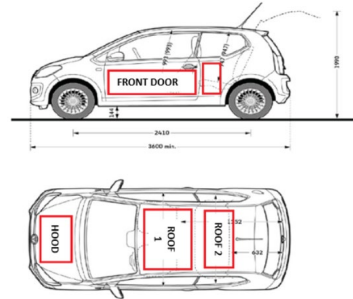


Figure 15. Example of maximum inscribable rectangle in Volkswagen Polo car body.

Segment	2022 sales	Tot. Area sheet used (10 <sup>3</sup> m <sup>2</sup> )	Tot. Area Al-sheet used (10 <sup>3</sup> m <sup>2</sup> )	Tot. Area steel-sheet used (10 <sup>3</sup> m <sup>2</sup> )	Al-sheet percentage (%)
A	199647	715,1	3,0	712,1	0,4
B	410767	2335,9	54,6	2301,4	2,3
C	255049	1385,3	89,4	1295,9	6,5
D	94038	657,8	119,3	538,5	18,1

Table 3. Al sheet percentage with respect to the total sheet used in the automotive field to produce external car body components.

Representative car model	Tot. Area from doors (m <sup>2</sup> )	Tot. Area from hood (m <sup>2</sup> )	Tot. Area from roof (m <sup>2</sup> )
UP (segment A)	1,03	0,24	0,86
T-Cross (segment B)	0,95	0,69	1,07
T-Roc (segment C)	1,33	0,49	0,71
Tiguan (segment D)	1,29	0,83	1,45

Table 4. Area of rectangular panels potentially recoverable by Volkswagen car models, representative of “common” and most-sold car designs in the Italian market.

By observing the data collected, it emerged that the most common Al component is the hood. This is because, as reported in [7], the transition from a steel hood to an aluminium one offers significant advantages.

Then, considering the Volkswagen brand as a representative brand (Table 2), for each segment, the average panel area present in the bodywork components (i.e. hood, roof, and doors) was calculated. Combining the data obtained from 2022 reference cars and the Volkswagen reference brand, the Al sheet percentage present in the car bodies of each segment (Table 3) is estimated. Making some assumptions on the likely gradual increase in the use of aluminium car body panels, the percentage of Al was calculated also for 2025. Finally, using again the Volkswagen brand as a



reference, for each segment, it was calculated the average surface achievable from each bodywork component (i.e. hood, roof, and doors) by determining the maximum inscribable rectangle in the car body (Figure 15). The achievable surface (Table 4) is intended as the sheet area that can be recovered from an ELV considering that in car bodies some obstacles to reworking such as handles, roof bars, cleaning systems for windscreen, etc. can be encountered.

Following this procedure, the aluminium output fluxes in 2040 can be calculated. The same route can be followed to calculate 2043 Al output fluxes with the expected 2025 aluminium percentage. A comparison between 2040 and 2043 Al sheet output fluxes was performed and the expected areas recoverable from the car body panels of ELVs are reported for three different market scenarios in Figure 16. It is worth noting that the quantity of recoverable Al sheets from ELVs is expected to increase exponentially, the figure proves that in only three years a growth of 81% might occur. The economic feasibility study was performed to evaluate if the remanufacturing of aluminium car body panels is a viable alternative to recycling from an economic perspective. Since remanufacturing through flattening is a novel recovery technique [1], different business scenarios were considered for the sake of completeness.

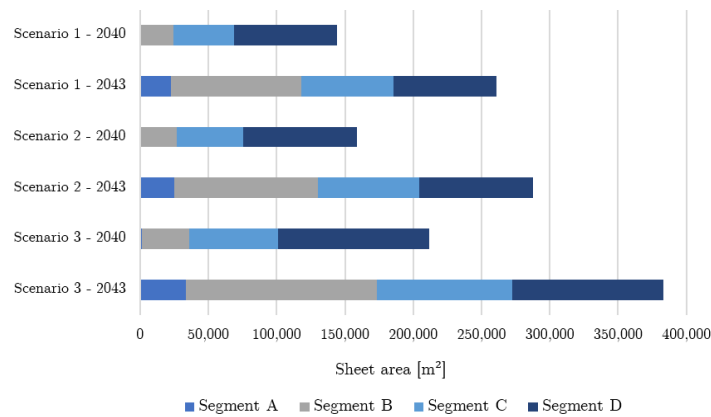


Figure 16. Predicted amounts of Al sheet from ELVs under three market scenarios.

A cost was calculated for each of the pre-flattening procedures, namely disassembly, cutting, polyurethane foam removal, paint stripping, and flattening costs. Other costs included in the analysis are opportunity costs. It is worth highlighting that the costs related to pre-flattening are unvaried for all the different scenarios. They have been calculated considering, for each different pre-flattening step, the contribution of three cost items: labour, equipment, and energy. The results obtained are 2.75 €/hood for the disassembly phase, 2.11 €/hood for the cutting operation, 2.50 €/hood for the polyurethane foam removal, and 7.80 €/hood for the paint stripping procedure performed with a chemical solvent. The total amounts to 15.16 €/hood. On the other hand, the costs related to the flattening operation vary depending on the business scenario considered and the expected Al sheet flux. For the first business scenario, it is assumed that the flattening is conducted by dismantlers who execute flattening on a rented press. In this case, the main cost items are the ones related to hoods transport and press renting, in addition to manpower and energy consumed by the press. The value of the energy consumed during each flattening cycle was obtained from the value of the instantaneous power consumed by the press. In a second business scenario, the possibility of integrating into the automotive market an emerging entity in charge of automotive sheet remanufacturing is assumed. Many assumptions were made, as having 20 sheet remanufacturers in the whole Italian area collaborating with the 1505 Italian authorized dismantlers. The costs to be calculated refer to hoods purchase, transport, manpower, energy, equipment, and facility. Summing up the pre-flattening costs to all the cost items generated by the flattening operation, the total costs of the remanufacturing procedure are obtained. The results are reported in Table 5 for 2040 and 2043,

crossing the business scenarios with the 3 above mentioned scenarios concerning to material fluxes. Another business scenario might consider that the flattening operations are performed by the Original Equipment Manufacturers (OEMs) or the Independent Remanufacturers (IRs). Recently, many automotive brands have introduced remanufacturing centres, however, they are all intended to remanufacture components that can be reused in car productions, not metal sheets [8]. For this reason, this scenario has not been further investigated.

Business scenarios	2040			2043		
	market scenarios			market scenarios		
	1	2	3	1	2	3
1	26.88 €	25.90 €	30.68 €	26.37 €	29.94 €	26.56 €
2	32.75 €	32.35 €	31.44 €	30.60 €	30.43 €	29.99 €

Table 5. Results of the cost analysis.

It is evident that the hood remanufacturing costs are bigger than the cost of a primary Al sheet of area equal to the one that can be obtained from an ELV hood, which is about 4 €. However, the remanufacturing costs are lower in 2043 than in 2040, this means that higher volumes of aluminium hoods incentivize this practice through a better cost amortization. Besides, we can expect, at least in Europe, increasing costs of critical raw materials; while at the moment the proposed process seems anti-economic, it provides a dramatic reduction of environmental impact, and it might economically benefit from future variation of the market and business conditions.

### Conclusions

In conclusion, the dies design phase allowed to create a re-forming instrument considering a multitude of design constraints. The technical feasibility allowed to define the best flattening parameters to achieve a uniform flattening. It is advisable to use high temperatures (250 °C), moderate pressures (30 MPa), and not excessively prolonged dwell times (10 s). Interrelationships between independent variables were also discovered, specifically between temperature and pressure, and between pressure and dwell time (Figure 10). Experimental observations also showed the complex deformation behaviour of sheets once flattened, showing an interesting spring-forward phenomenon. Moreover, the simulation on Altair Inspire Form proved that the flattening process does not highly compromise the material formability (Figure 13) and that digital tools can be used for predicting the final part geometry (Figure 11). The economic feasibility analysis enabled to evaluate the costs related to five different remanufacturing business scenarios. The most viable scenarios emerged: flattening performed by dismantlers who rent the press and flattening executed by new remanufacturing figures. However, the costs associated with Al hoods remanufacturing are high (Table 5), surpassing the costs of purchasing new aluminium sheets of the same area amounting to 4 €. Therefore, only a significant growth in Al hood volumes and the introduction of governmental incentives can make aluminium hoods remanufacturing become advantageous. From the analysis performed on the possible future Al fluxes generated by ELVs, it can be stated that, if aluminium will be introduced in bodywork components more massively, as stated by many car brands, an exponential growth in Al sheet volumes is expected. By simply assuming that, in 2025, aluminium hoods will be introduced in some of the best-selling car models of 2022, the volumes of Al achievable from ELVs would nearly duplicate passing from 2040 to 2043.

### References

[1] D. Farioli, M. Fabrizio, E. Kaya, M. Strano, and V. Mussi, “Reshaping of thin steel parts by cold and warm flattening,” *Int. J. Mater. Form.*, vol. 16, no. 4, 2023. <https://doi.org/10.1007/s12289-023-01759-y>

- [2] J. R. Duflou *et al.*, “Environmental assessment of solid state recycling routes for aluminium alloys: Can solid state processes significantly reduce the environmental impact of aluminium recycling?,” *CIRP Ann. - Manuf. Technol.*, vol. 64, no. 1, pp. 37–40, 2015. <https://doi.org/10.1016/j.cirp.2015.04.051>
- [3] D. Parker *et al.*, “Remanufacturing Market Study,” 2015.
- [4] A. Shahedi, M. M. Nasiri, M. S. Sangari, F. Werner, and F. Jolai, “A Stochastic Multi-Objective Model for a Sustainable Closed-Loop Supply Chain Network Design in the Automotive Industry,” *Process Integr. Optim. Sustain.*, vol. 6, no. 1, pp. 189–209, Mar. 2022. <https://doi.org/10.1007/s41660-021-00204-4>
- [5] G. Copani, P. Shafinejad, T. Hipke, R. Haase, and T. Paizs, “New metals remanufacturing business models in automotive industry,” *Procedia CIRP*, vol. 112, pp. 436–441, 2022. <https://doi.org/10.1016/j.procir.2022.09.033>
- [6] F. Grimaldi, “Erase & Rewind,” Politecnico di Milano, 2022.
- [7] M. A. Omar, *The Automotive Body Manufacturing Systems and Processes*. Wiley, 2011. doi: 10.1002/9781119990888
- [8] M. Kalverkamp and T. Raabe, “Automotive Remanufacturing in the Circular Economy in Europe,” *J. Macromarketing*, vol. 38, no. 1, pp. 112–130, Mar. 2018. <https://doi.org/10.1177/0276146717739066>